

WASHINGTON UNIVERSITY  
DEPARTMENT OF PHYSICS  
LABORATORY FOR ULTRASONICS  
St. Louis, Missouri 63130

189385  
15P

**"Physical Interpretation and Development of Ultrasonic Nondestructive  
Evaluation Techniques Applied to the Quantitative Characterization of Textile  
Composite Materials"**

Semiannual Progress Report: March 15, 1993 - September 14, 1993

NASA Grant Number: NSG-1601

N94-15190  
Unclas  
0189385

Principal Investigator:

Dr. James G. Miller  
Professor of Physics

The NASA Technical Officer for this grant is:

Dr. Joseph S. Heyman  
NASA Langley Research Center  
Hampton, Virginia

(NASA-CR-194549) PHYSICAL  
INTERPRETATION AND DEVELOPMENT OF  
ULTRASONIC NONDESTRUCTIVE  
EVALUATION TECHNIQUES APPLIED TO  
THE QUANTITATIVE CHARACTERIZATION  
OF TEXTILE COMPOSITE MATERIALS  
Semiannual Progress Report, 15 Mar. 1993  
- 14 Sep. 1993 (Washington Univ.)  
15 p

## **Introduction**

In this Progress Report, we describe our current research activities concerning the development and implementation of advanced ultrasonic nondestructive evaluation methods applied to the characterization of stitched composite materials and bonded aluminum plate specimens. One purpose of this investigation is to identify and characterize specific features of polar backscatter interrogation which enhance the ability of ultrasound to detect flaws in a stitched composite laminate. Another focus is to explore the feasibility of implementing medical linear array imaging technology as a viable ultrasonic-based nondestructive evaluation method to inspect and characterize bonded aluminum lap joints. As an approach to implementing quantitative ultrasonic inspection methods to both of these materials, we focus on the physics that underlies the detection of flaws in such materials.

## **Measurements of Stitched Composites with 3D Architecture**

In this section of the Progress Report we describe the experimental methods applied and the resultant data obtained from through-transmission and polar backscatter measurements of a set of stitched composite samples.

### **Samples**

A total of four stitched composite plate samples were investigated in this study. Each composite sample was comprised of a series of woven carbon/epoxy sheets laid-up in a 0°/45°/90° pattern. The plates had Kevlar™ stitching running perpendicular to the laminae and the front and back surfaces of each plate were machined smooth to remove any surface impressions.

Three of the samples (labeled 2150-3-CAI1, 2150-3-CAI2, and 2150-3-CAI3) were cut from a single large piece of material that had previously been impact-damaged at one end. The samples were cut from the end of this large piece opposite the region of impact, where there was presumably no damage. The samples were labeled on one side, indicating where the impact damage had occurred. Each of these samples measured approximately 4" x 5" with a thickness of 0.075". The stitches in these samples appeared to be approximately 0.025" (1mm) in diameter, and were spaced in a grid-like pattern with 4mm to 6mm separation between successive stitches.

The fourth sample (labeled 2130-7-CA11) was cut from the undamaged portion of a separate large plate of impacted composite material. This sample measured 4" x 5" with a thickness of 0.275". The stitches in this sample appeared to be about 0.075" (2mm) in diameter, and were spaced in a grid-like pattern with 4mm to 6mm separation between stitches. The surface of this sample had a different appearance than the three thinner samples described above; for this sample, the stitches were a different color and the stitched areas were somewhat oblong in shape. The pattern of the carbon fiber tows on the front and back surfaces also appeared to be more complex with this sample than with the thinner samples. This may be due to a different weave pattern used in the laminae for this particular sample.

### **Experimental Set-Up and Procedure**

Initially, a through-transmission C-scan was performed on each sample to determine if the plates had any internal delaminations, nonuniformities, or porosity. All measurements were performed in an immersion tank using Panametrics V311 0.5" diameter, point-focused (4") piezoelectric transducers of 10 MHz nominal center frequency. For the through-transmission C-scans, the samples were positioned such that the front surface was 4" away from the transmitting transducer and the matched receiving transducer was placed 8" away from the transmitting transducer. Transmitted ultrasonic signals were broadband pulses generated by a Panametrics 5800 Pulser/Receiver. Each through-transmitted pulse was captured by the receiving transducer, amplified and filtered by the receiver section of the Panametrics 5800, and subsequently sent to a Tektronix 2430a digital oscilloscope for digitization. The peak-to-peak signal voltage amplitude at each site was stored on a Macintosh IIX computer.

A polar backscatter investigation was performed on one of the thinner samples (2150-3-CA11). A Panametrics V311 0.5" diameter, point-focused (4") piezoelectric transducer of 10 MHz nominal center frequency was used to transmit and receive the ultrasonic signal. The transducer was positioned at a polar angle of 30° (the azimuthal angle was varied), with the axis 4" away from the top surface of the sample. Figure 1 illustrates the transducer position in relation to the sample. Transmitted ultrasonic signals were broadband pulses generated by a Panametrics 5800 Pulser/Receiver. The backscattered ultrasonic signals were received by the transmitting/receiving transducer, amplified and filtered by the receiver section of the Panametrics 5800, and sent to a Tektronix 2430a digital oscilloscope for digitization. A total of 20  $\mu$ s of the backscattered signal was digitized at 50 megasamples/sec. The rf signal at each site was stored on a Macintosh IIX computer. For each data run, a reference signal was obtained by capturing the signal reflected from a stainless-steel plate. Data analysis proceeded as follows: at

# Polar Backscatter Method

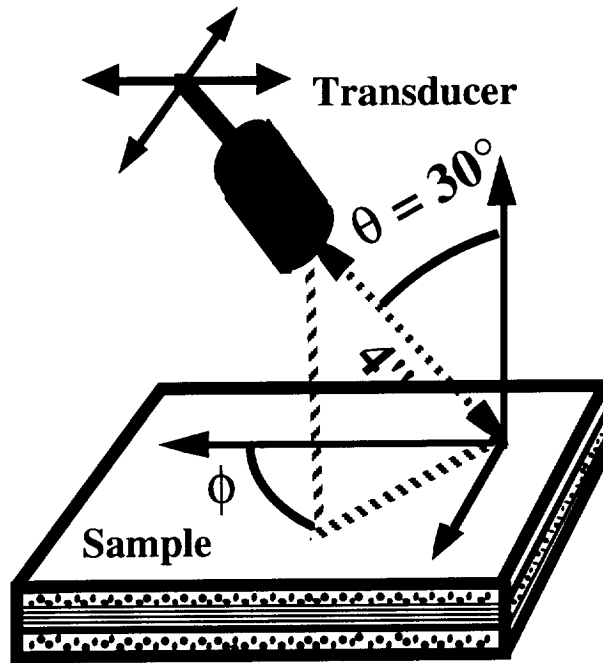
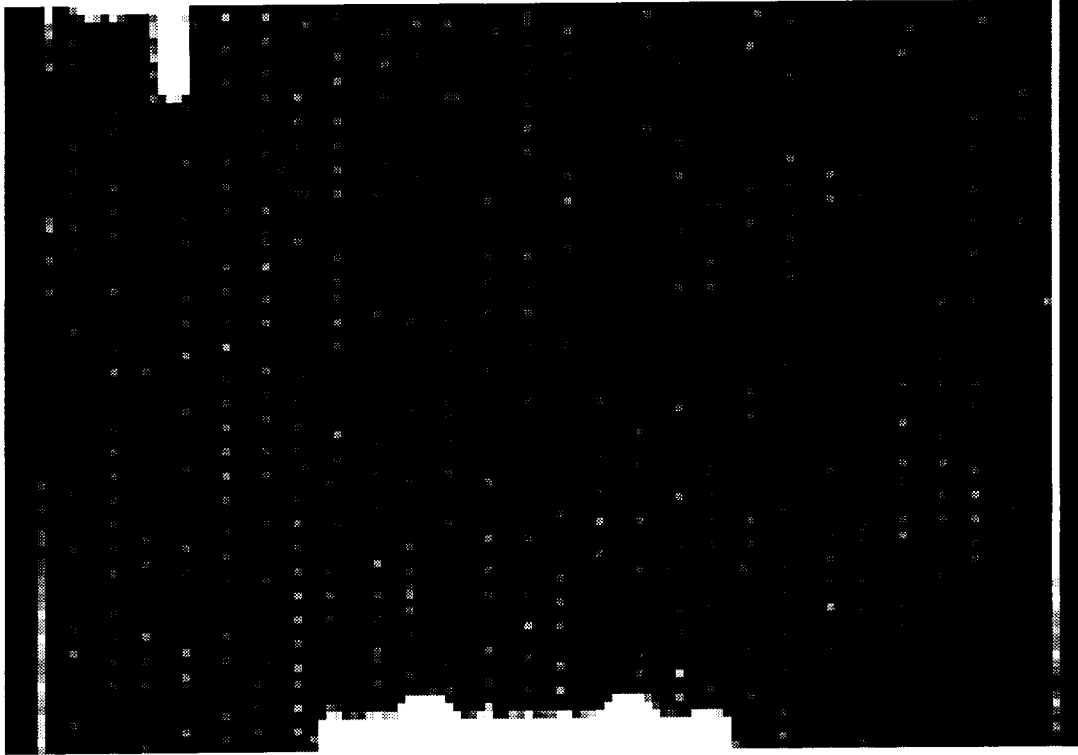


**Figure 1.** Schematic diagram showing transducer and sample orientation for polar backscatter experiment.

each interrogated site the power spectrum corresponding to the reference signal (expressed in dB) was subtracted from the power spectrum corresponding to backscattered signal from the sample (also in dB) thus giving the apparent backscatter transfer function. This process is employed to deconvolve the response of the equipment from the measured backscattered signal. The resulting backscatter transfer function was then averaged (in the log domain) from 4 to 8 MHz to obtain a single parameter (integrated backscatter) for each site.

## Results

Through-transmission peak-to-peak signal-loss images of all four samples are shown in Figures 2 through 5. Step sizes for each of the scans was 1mm x 1mm. A tape marker was adhered to the upper left corner of each sample thus providing a reference position in each image. The areas that appear darker correspond to regions of less signal loss compared to the lighter areas. The pattern of light spots in each image corresponds to the stitching in the plate;



## Schematic

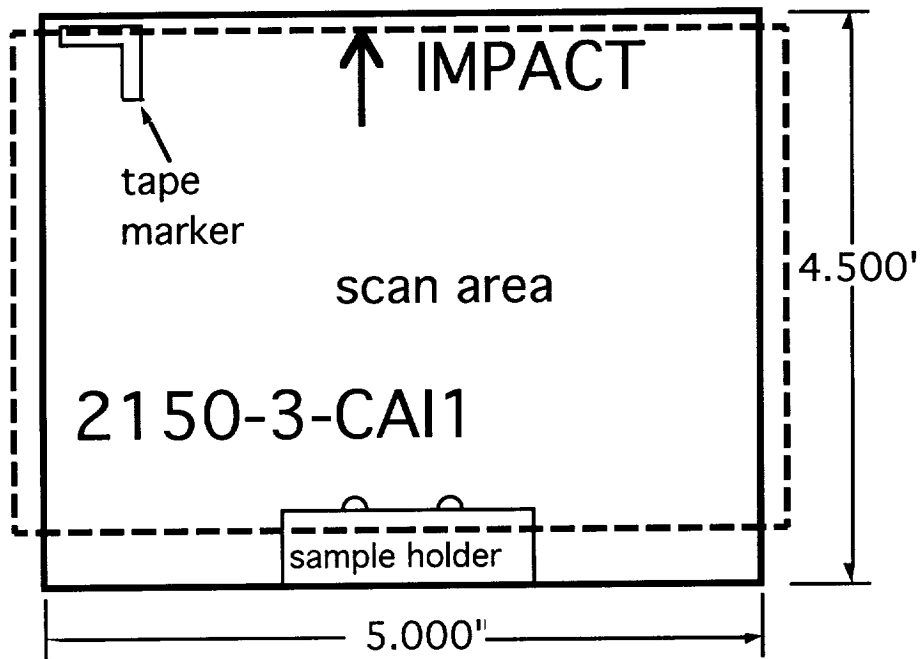
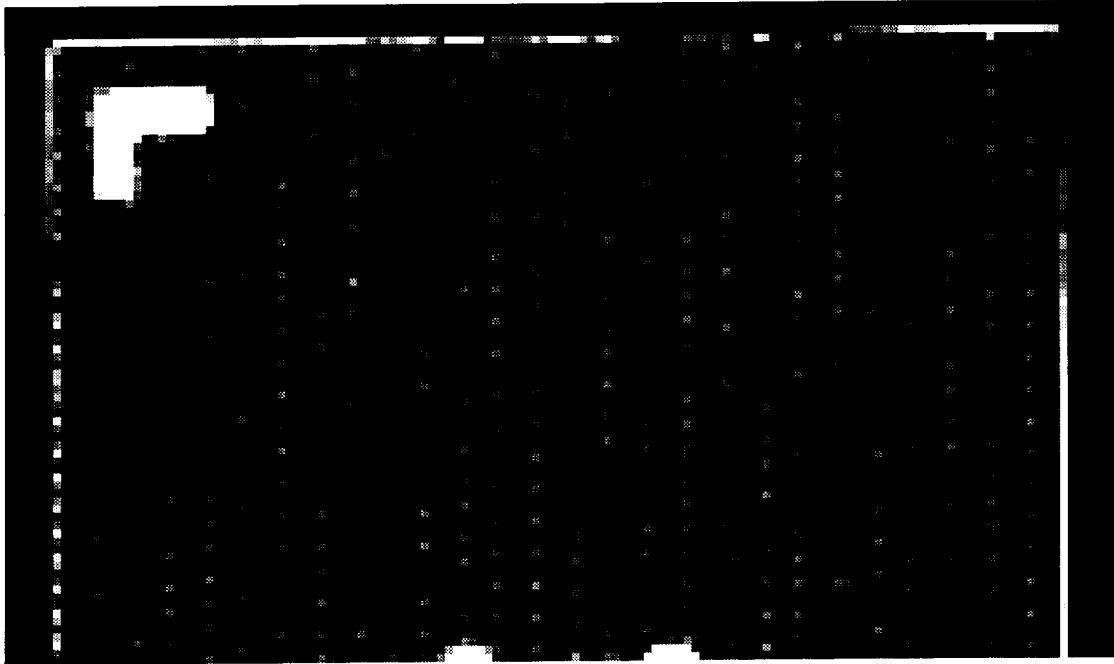


**Figure 2.** Sample: 2150-3-CAI1, stitched quasi-isotropic composite, 4.5"x5"x0.07", surfaces ground smooth. Through-transmission C-scan, 10 MHz, 0.5" diameter transducers with 4" focal length; 135 x 93 sites, 1mm stepsize. Image shows peak-to-peak values.



### Schematic

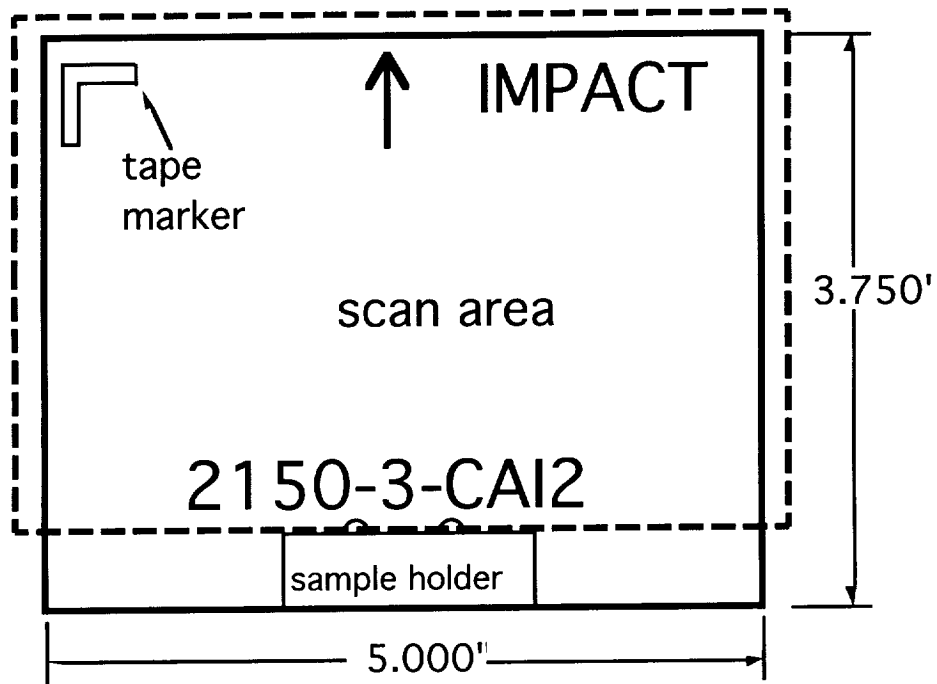
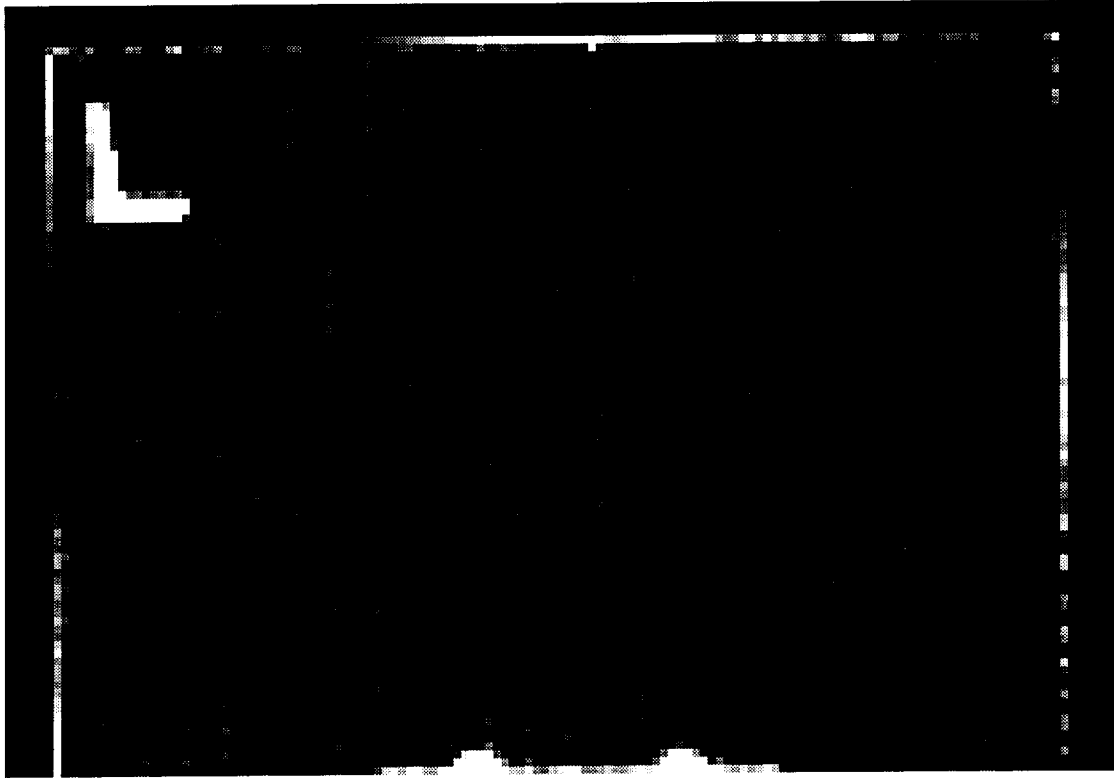


**Figure 3.** Sample: 2150-3-CAI2, stitched quasi-isotropic composite, 3.75"x5"x0.07", surfaces ground smooth. Through-transmission C-scan, 10 MHz, 0.5" diameter transducers with 4" focal length; 139 x 82sites, 1mm stepsize. Image shows peak-to-peak values.



### Schematic

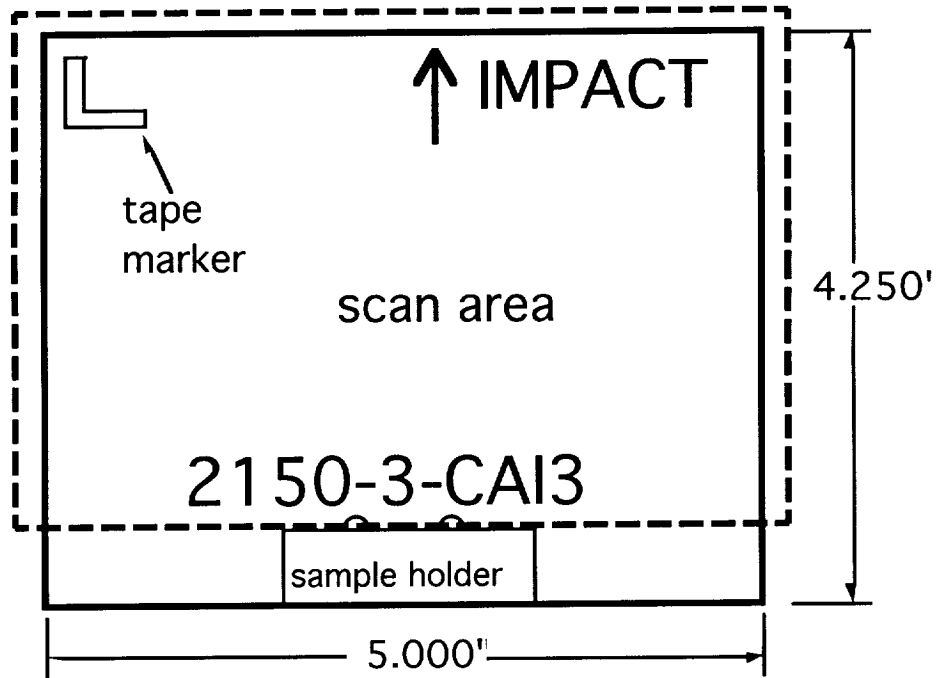
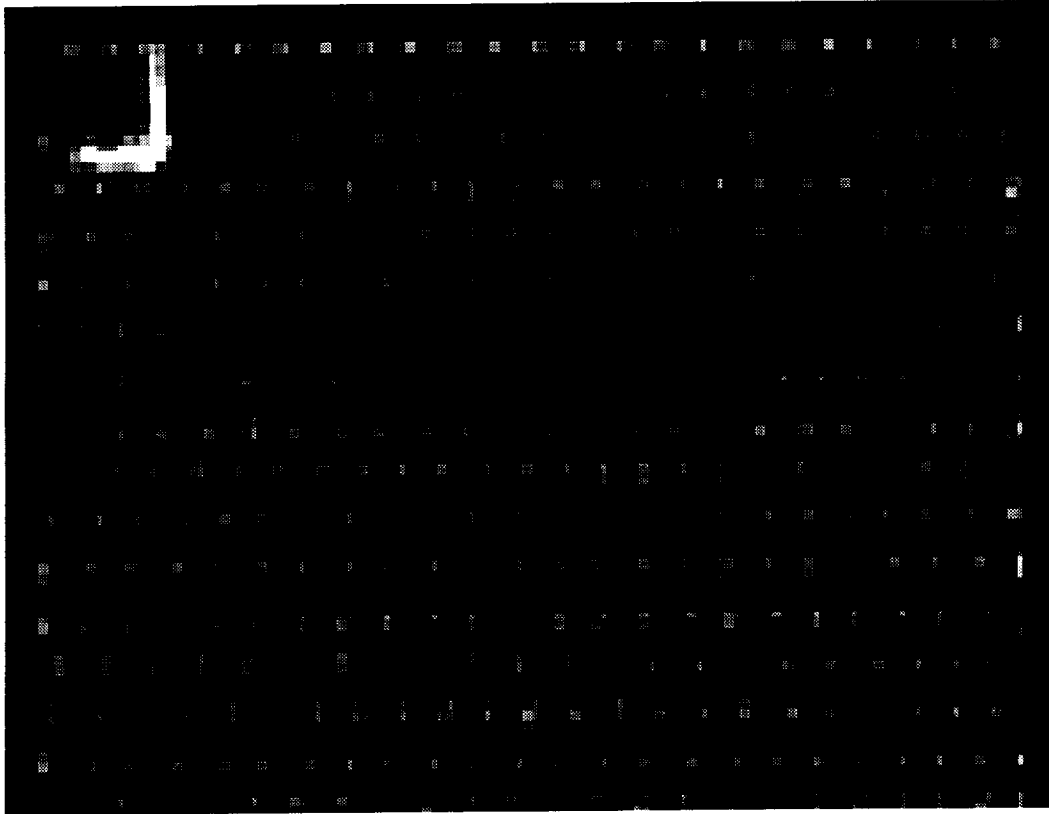


**Figure 4.** Sample: 2150-3-CAI3, stitched quasi-isotropic composite, 4.25"x5"x0.07", surfaces ground smooth. Through-transmission C-scan, 10 MHz, 0.5" diameter transducers with 4" focal length; 139 x 96 sites, 1mm stepsize. Image shows peak-to-peak values.



## Schematic

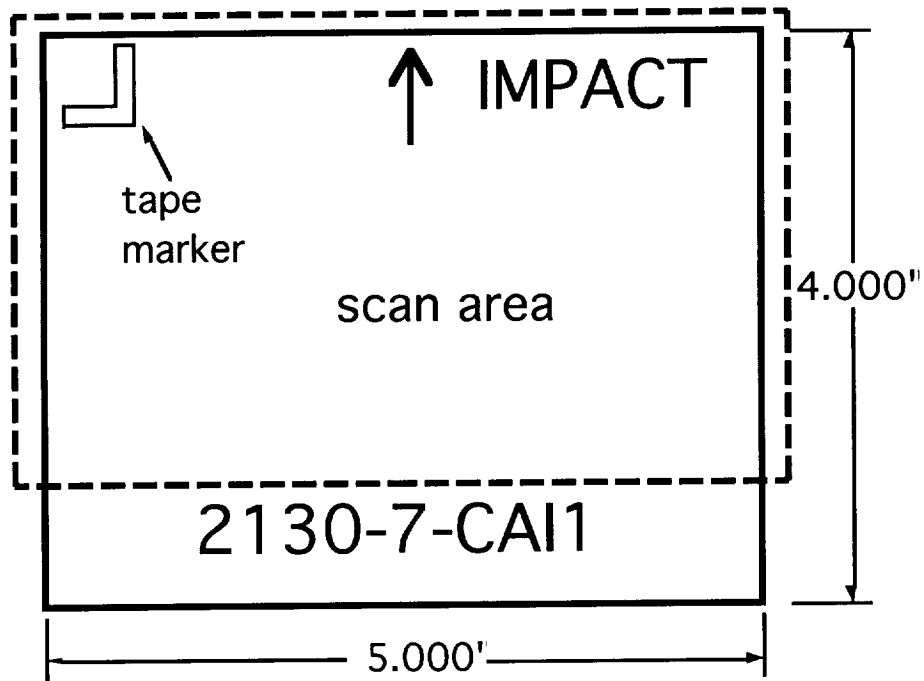


**Figure 5.** Sample: 2130-7-CAI1, stitched quasi-isotropic composite, 4"x5"x0.25", surfaces ground smooth. Through-transmission C-scan, 10 MHz, 0.5" diameter transducers with 4" focal length; 135 x 83 sites, 1mm stepsize. Image shows peak-to-peak values.

less of the signal appeared to get through the Kevlar™ stitched region compared to the amount of signal transmitted through the carbon/epoxy. With the exception of the areas near the stitches, the images all seem to be fairly uniform in gray-scale, suggesting that there are no gross defects (i.e. porosity, delaminations, etc.) in the samples.

Polar backscatter C-scans performed on sample 2150-3-CA11, at a polar angle of 30° and varying azimuthal angles, are shown in Figure 6. The region interrogated was the same area inspected with through-transmission signal loss as described above. The step size was 0.5mm x 0.5mm, and the total scan area was 20mm x 20mm. In all the integrated backscatter images, white corresponds to a value of -50dB below the reference signal from the stainless-steel plate, and black corresponds to -30 dB below the stainless-steel plate reference. A stitch-like pattern of dark (high-scattering) spots is clearly discernible in specific images (at azimuthal angles of 22°, 67°, and 202°). It has been shown previously that backscatter from the carbon fibers in a composite laminate is minimized when the azimuthal angle of insonification is parallel to the fiber direction and a maximum when the azimuthal angle of insonification is perpendicular to the fiber direction.[1-6] Thus, one might expect to see the least amount of backscatter arising from the embedded carbon fibers to occur at azimuthal angles that are furthest from being perpendicular to the fiber direction in any layer; however, the backscatter from the stitches should be isotropic with respect to azimuthal angle. Therefore, the greatest contrast between stitches and embedded carbon fibers should occur at angles where the contribution to the scattered signal from the embedded fibers is the least. Evidence of this can be seen in the images for angles 22°, 67° and 202°, where the stitch pattern is most easily distinguished from the surrounding material and is consistent with the quasi-isotropic lay-up of this specimen. The stitched areas in the images appear to be 3 to 6 pixels (1.5mm to 3mm) in diameter. This may be due to changes in the material around the stitches, or to the point spread function of the interrogating beam, which had a -6dB beam width of 1.2mm.

Anisotropy scans were performed on a stitched region and a non-stitched region of sample 2150-3-CA11 with a polar angle of 30°. At every azimuthal angle (varied in 2° steps), nine site averages were taken. Figure 7 shows integrated backscatter (4 to 8 MHz) plotted vs azimuthal angle for both regions (stitched and non-stitched). The curves appear similar except at the angles 22° and 202°, where the contrast between the stitches and fibers is greatest.

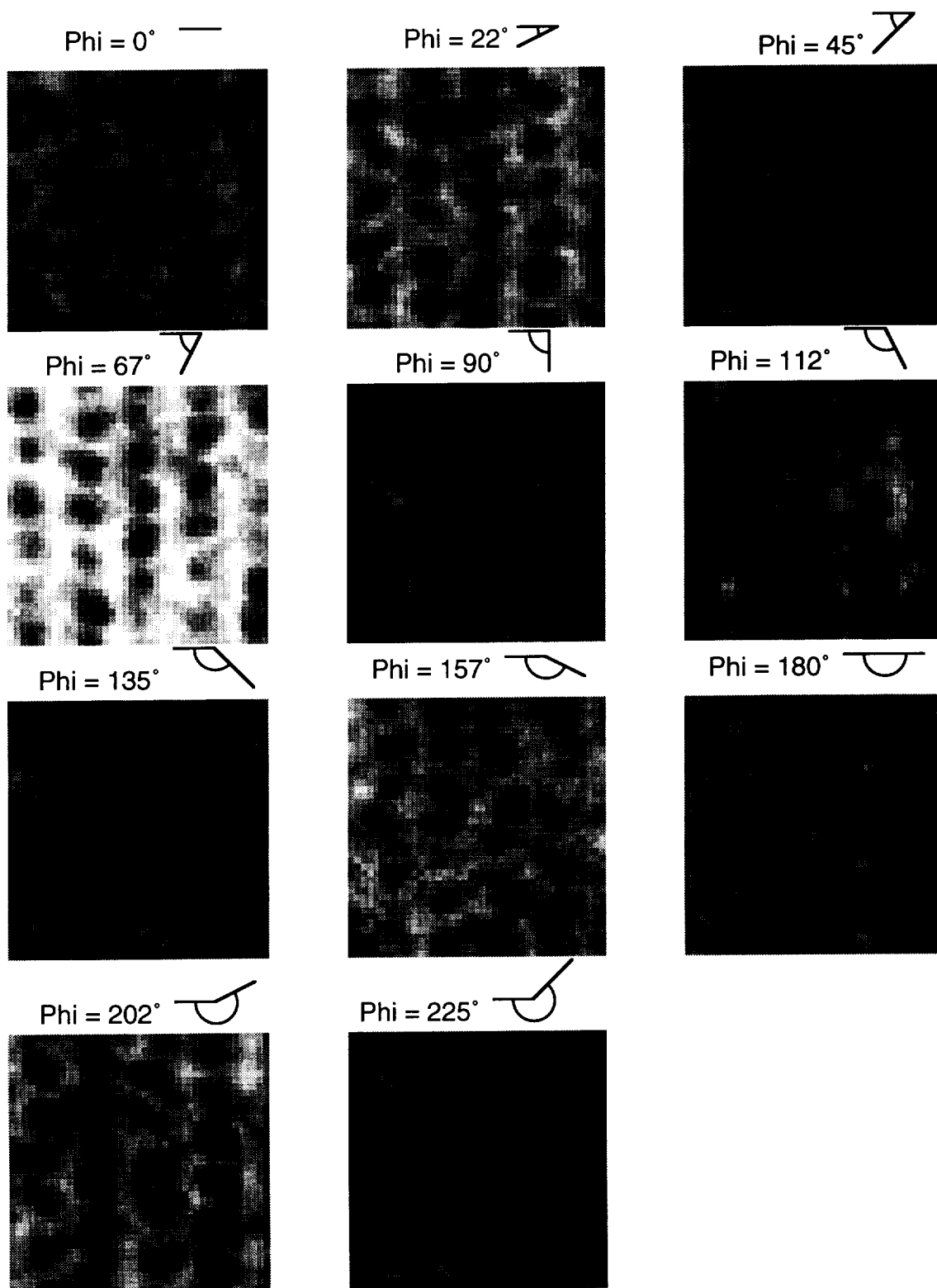


**Figure 6:** Polar integrated backscatter images (4 to 8 MHz) from sample 2150-3-CA11. Polar angle Theta = 30°

## Anisotropy of Integrated Backscatter Sample 2150-3-CAI1

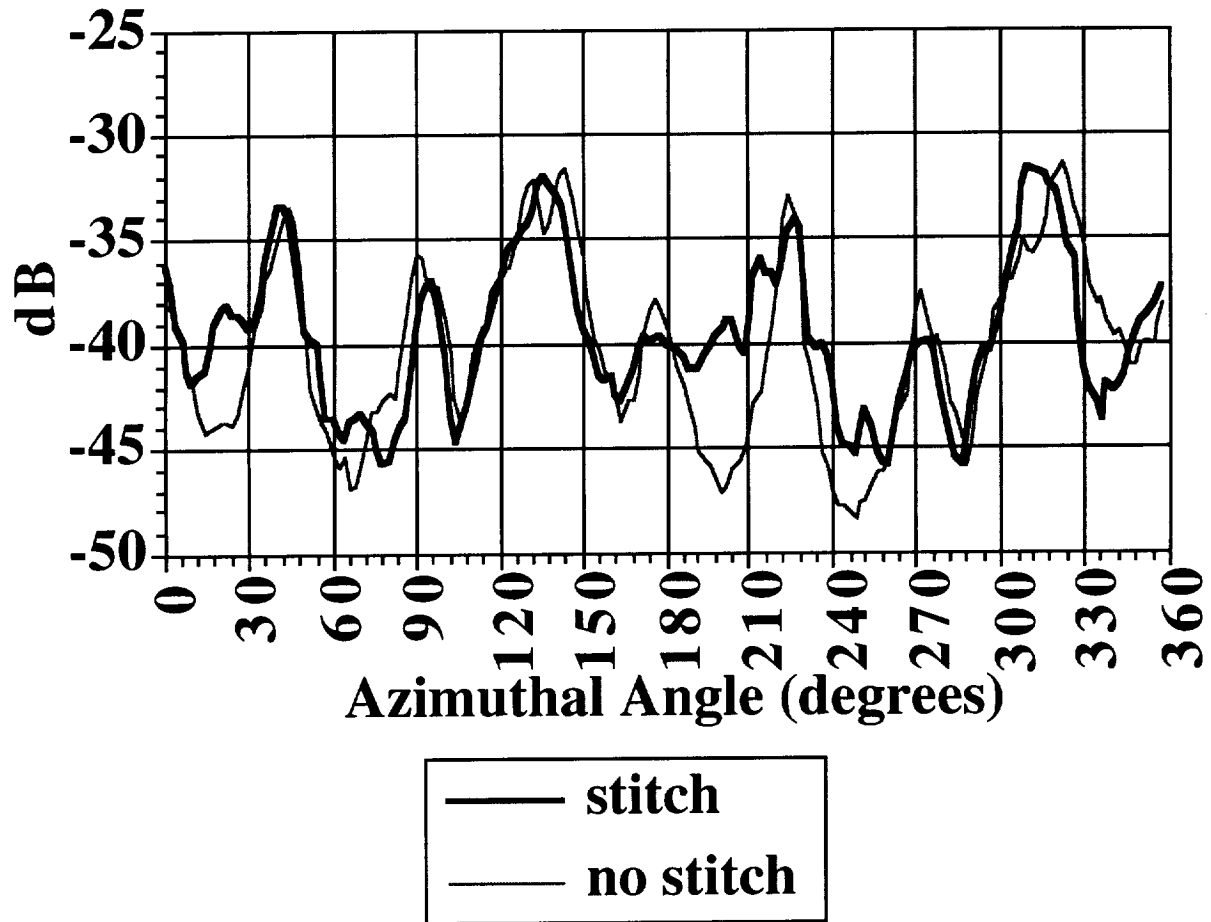


**Figure 7.** Integrated backscatter (4 to 8 MHz) plotted vs azimuthal angle for both regions (stitched and non-stitched).

# **Detection of Disbonded Regions in Bonded Aluminum Plates Using an Ultrasonic 7.5 MHz Linear Array Medical Imaging System**

## **Introduction**

Current concern for ensuring the air-worthiness of the aging commercial air fleet has prompted the establishment of broad-agency programs to develop NDT technologies that address specific aging-aircraft issues.[7, 8] One of the crucial technological needs that has been identified is the development of rapid, quantitative systems for depot-level inspection of bonded aluminum lap joints on aircraft.[7-9] Research results for characterization of disbond and corrosion based on normal-incidence pulse-echo measurement geometries are showing promise, but are limited by the single-site nature of the measurement which requires manual or mechanical scanning to inspect an area.[10-13] One approach to developing efficient systems may be to transfer specific aspects of current medical imaging technology to the NDT arena. Ultrasonic medical imaging systems offer many desirable attributes for large scale inspection. They are portable, provide real-time imaging, and have integrated video tape recorder and printer capabilities available for documentation and post-inspection review. Furthermore, these systems are available at a relatively low cost (approximately \$50,000 to \$200,000) and can be optimized for use with metals with straight-forward modifications. As an example, ultrasonic phased-array and linear array imaging technology, which was first developed for use in the medical industry, has been successfully implemented for some NDT applications by other investigators.[14-16]

Currently, we are engaged in an investigation that explores the feasibility of implementing medical linear array imaging technology as a viable ultrasonic-based nondestructive evaluation method to inspect and characterize bonded aluminum lap joints. Images of a series of epoxy-bonded aluminum plate specimens, each with intentionally disbonded regions (adhesive tape), were obtained using an unmodified, commercially-available Hewlett-Packard SONOS 1500 medical imaging system. Because of the nature of detecting disbonded regions in relatively thin aluminum specimens, the SONOS 1500 imaging system was operated in a mode normally employed to image peripheral blood vessels in a clinical setting. These images were compared with corresponding conventional ultrasonic contact transducer measurements in order to assess whether these images can detect disbonded regions and provide information regarding the nature of the disbonded region. The results of this investigation may provide a step toward the development of a rapid, real-time, and portable method of adhesive bond inspection and characterization based on linear array technology.

## Discussion

Preliminary results, comparing the images of the bonded aluminum plate specimens obtained with the linear array with the corresponding ultrasonic rf A-lines obtained using a contact transducer, suggest that linear array imaging can play a useful role in detecting disbanded regions and providing information describing bond interface characteristics. The disbanded regions were easily discernible from the well-bonded regions in the images obtained from either side of each specimen. Images of the specimens show that the disbanded regions appear much different when the images obtained from the "bottom" of the specimen are compared with those obtained from the "top". Our preliminary results show that a relatively "bright" disbond region observed when the specimens are imaged from the "bottom" side and a "dark" disbond region observed when the specimens are imaged from the "top" side agree with the corresponding echo decay patterns obtained with the contact transducer; i.e., a relatively higher attenuation associated with the disbanded region when interrogated from the "top" when compared with the results obtained from the "bottom". Subsequent destructive analysis of the specimens indicated that the "bottom" plate was in direct contact with the adhesive of the masking tape (as expected) but the "top" plate had a thin substance adhered to it. These preliminary results suggest that the images obtained with the linear array may convey information regarding the characteristics of the interface between the aluminum and the disbond.

Many aspects of the images of the well-bonded regions of the specimens obtained with the SONOS 1500 linear array are consistent with the contact transducer data. Modulations of the brightness of the well-bonded region in the images of specific specimens agree with the observed modulations in the echo decay patterns obtained with the contact transducer. Image patterns of specimens that have aluminum plates of different thicknesses are consistent with the measured rf A-lines of these specimens. The images and corresponding rf A-lines of these specimens show that the well-bonded regions appear different when interrogated from the "bottom" side and compared with the image from the "top" side. This difference between the two sides is evident in the measured echo decay patterns obtained.

These preliminary measurements, showing the linear-array images of the bonded aluminum plate specimens and the corresponding agreement with contact transducer measurements, suggest that linear array technology may provide a viable means to detect disbanded regions in bonded aluminum joints. Furthermore, these images may provide useful information regarding the nature of the disbanded region. It appears that medical linear array imaging technology may offer a useful means to develop a rapid, real-time, and portable method of adhesive bond inspection and characterization.

## References

1. Blodgett, E.D., S.M. Freeman, and J.G. Miller, *Correlation of Ultrasonic Polar Backscatter With the Depty Technique for Assessment of Impact Damage in Composite Laminates*. Review of Progress in Quantitative Nondestructive Evaluation, 1986. **5B**: p. 1227-1238.
2. Blodgett, E.D., L.J. Thomas III, and J.G. Miller, *Effects of Porosity on Polar Backscatter From Fiber Reinforced Composites*. 1986. **5B**: p. 1267-1274.
3. Handley, S.M., J.G. Miller, and E.I. Madaras. *An Investigation of the Relationship Between Contrast and Azimuthal Angle for Imaging Porosity in Graphite/Epoxy Composites with Ultrasonic Polar Backscatter*. in *Proc. IEEE Ultrasonics Symposium*. 1988. Chicago: Vol. **88 CH 2578-3**, 1031-1034
4. Handley, S.M., J.G. Miller, and E.I. Madaras. *Effects of Bleeder Cloth Impressions on the Use of Polar Backscatter to Detect Porosity*. in *Review of Progress in QNDE*. 1988. La Jolla: Plenum Press. Vol. **8B**, 1581-1587
5. Smith, B.T., *et al.*, *Correlation of the Depty Technique With Ultrasonic Imaging of Impact Damage in Graphite-Epoxy Composites*. Materials Evaluation, 1989. **47**: p. 1408-1416.
6. Thomas, L.J., III, E.I. Madaras, and J.G. Miller. *Two-Dimensional Imaging of Selected Ply Orientations in Quasi-Isotropic Composite Laminates Using Polar Backscattering*. in *Proc. IEEE Ultrasonics Symposium*. 1982. San Diego: Vol. **82 CH 1823-4**, 965-970
7. Bobo, S.N. *The Aging Aircraft Fleet: A Challenge for Nondestructive Inspection*. in *Review of Progress in Quantitative Nondestructive Evaluation*. 1990. Brunswick, ME: Plenum Publishing Corporation. Vol. **9**, 2097-2109
8. Seher, C. and A.L. Broz, *National Research Program for Nondestructive Inspection of Aging Aircraft*. Materials Evaluation, 1991. **49**(12 (December)): p. 1547-1550.
9. Iddings, F.A. *Large-Area Aircraft Scanner*. in *Review of Progress in Quantitative Nondestructive Evaluation*. 1992. Brunswick, ME: Plenum Publishing Corporation. Vol. **11**, 2233-2240
10. Patton, T.C. and D.K. Hsu. *Ultrasonic NDE of Adhesive and Sealant Bonded Aluminum Lap Joints*. in *Review of Progress in Quantitative Nondestructive Evaluation*. 1992. Brunswick, ME: Plenum Publishing Corporation. Vol. **11**, 1299-1306
11. Hsu, D.K., M.S. Hughes, and T.C. Patton. *Ultrasonic Scans Using Low Frequency Unresolved Echoes*. in *Review of Progress in Quantitative Nondestructive Evaluation*. 1993. Brunswick, ME: Plenum Publishing Corporation. Vol. **12**, 1595-1602
12. Abedin, M.N., *et al.* *A Comparative Study of Experimental and Simulated Ultrasonic Pulse-Echo Signals from Multilayered Structures*. in *Review of Progress in Quantitative Nondestructive Evaluation*. 1992. Brunswick, ME: Plenum Publishing Corporation. Vol. **11**, 1959-1966
13. Abedin, M.N., P.H. Johnston, and D.R. Prabhu. *Disbond Detection Using Peak Amplitude of Pulse-Echo Signals for Various Thicknesses and Transducer Frequencies*. in *Review of Progress in Quantitative Nondestructive Evaluation*. 1993. Plenum Publishing Corporation. Vol. **12**, 1539-1546

14. Dunki-Jacobs, R. and L.J. Thomas. *Real-Time B-Scan Ultrasonic Imaging Using a Digital Phased Array System for NDE*. in *Review of Progress in Quantitative Nondestructive Evaluation*. 1992. Brunswick, ME: Plenum Publishing Corporation. Vol. **11**, 805-812
15. Wustenberg, H., *et al.*, *Ultrasonic Phased Arrays for Nondestructive Inspection of Forgings*. *Materials Evaluation*, 1993. **51**(6 (June)): p. 669-812.
16. Posakony, G.J. *Acoustic Imaging - A Review of Current Techniques for Utilizing Ultrasonic Linear Arrays for Producing Images of Flaws in Solids*". in *Elastic Waves and Non-Destructive Testing of Materials (ASME-AMD)*. 1978. Vol. **29**, 53 -69